

Stereoisomer Effects on the Paal-Knorr Synthesis of Pyrroles<sup>1</sup>

Gyöngyi Szakál-Quin and Doyle G. Graham\*

Department of Pathology, Duke University Medical Center, Durham, North Carolina 27710

David S. Millington and David A. Maltby

Division of Genetics and Metabolism, Department of Pediatrics, Duke University Medical Center, Durham, North Carolina 27710

Andrew T. McPhail

Gross Chemical Laboratory, Duke University, Durham, North Carolina 27710

Received July 19, 1985

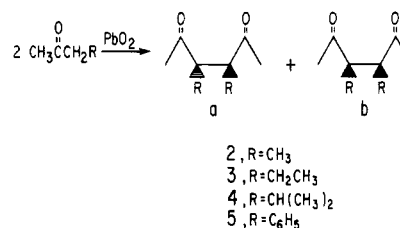
The neurotoxicity of *n*-hexane has been postulated to result from the reactivity of its  $\gamma$ -diketone metabolite, 2,5-hexanedione (1), with lysyl amino groups of proteins to form pyrroles (Paal-Knorr synthesis). We have synthesized a series of 3,4-disubstituted  $\gamma$ -diketones in order to explore the relationship between rate of pyrrole formation and neurotoxicity. The  $\gamma$ -diketones were prepared through oxidative coupling of ketones. Yields were improved to 60–70% with the use of a Soxhlet apparatus containing PbO<sub>2</sub> in the extraction thimble. Diketones prepared were 3,4-dimethylhexane-2,5-dione (2), 3,4-diethylhexane-2,5-dione (3), 3,4-diisopropylhexane-2,5-dione (4), and 3,4-diphenylhexane-2,5-dione (5). The reactions yielded mixtures of the *d,l* (a) and meso (b) diastereomers, which were separated by column chromatography, fractional distillation, or crystallization. Structures of the diastereomeric forms were established by <sup>13</sup>C NMR techniques and, in the case of 4b, by single-crystal X-ray diffraction. The relative reactivities of the *d,l* and meso isomers of each  $\gamma$ -diketone were determined with benzylamine in cyclohexane and the rate of pyrrole formation was determined by HPLC. For each pair of diastereomeric diketones the *d,l* reacted 4–40 times faster than the meso form. The reactivities of the  $\gamma$ -diketones were in the order 2 > 1 > 3 > 5 > 4 with pseudo-first-order rate constants ranging from 4 × 10<sup>-4</sup> to 3 × 10<sup>-8</sup> s<sup>-1</sup> at 30 °C.

The neurotoxicity of *n*-hexane has been postulated to result from the reactivity of its  $\gamma$ -diketone metabolite, 2,5-hexanedione (1), with lysyl amino groups of proteins to form pyrroles.<sup>2</sup> Both rate of pyrrole formation with amines and neurotoxicity of 1 were enhanced by 3,4-dimethyl substitution.<sup>3</sup> In concept, 3,4-disubstitution could accelerate or impair the rate of pyrrole formation, depending upon the size of the substituent and its *d,l* or meso conformation. In this study we have synthesized and separated both the *d,l* and meso isomers of 3,4-dimethylhexane-2,5-dione (2), 3,4-diethylhexane-2,5-dione (3), 3,4-diisopropylhexane-2,5-dione (4), and 3,4-diphenylhexane-2,5-dione (5) in order to characterize stereoisomer effects on the Paal-Knorr synthesis of pyrroles.<sup>4</sup>

## Results and Discussion

The 3,4-disubstituted  $\gamma$ -diketones were prepared through oxidative coupling of ketones.<sup>5</sup> This reaction is usually conducted by heating the ketone with a suspension of lead(IV) oxide, but we found that yields could be improved (60–70%) by refluxing the ketone through a thimble containing PbO<sub>2</sub> in a Soxhlet apparatus. By this technique, the  $\gamma$ -diketone product is largely protected from further oxidation. The reactions gave mixtures of *d,l* (a) and meso (b) diastereomers, which were separated by column chromatography, fractional distillation, or fractional crystallization.

Previous studies have succeeded in separating the diastereomers of 2<sup>6,7</sup> and 5<sup>6</sup> with proof of structure established in each case. However, synthesis, purification, and structural verification had not been accomplished for 3 or 4 diastereomers. One report<sup>8</sup> gave <sup>1</sup>H NMR spectra for "isomers" of 3, but these were not further identified.



In the present studies, lower retention times on gas chromatography and lower boiling or melting points were used initially to distinguish *d,l* (a) from meso (b) diastereomers (Table I). Mass spectral analyses were performed on each diastereomer during combined gas chromatography-mass spectrometry, yielding the expected molecular ion and fragmentation. In general, the *d,l* pair exhibited more abundant M<sup>+</sup> ions and primary fragment ions than the corresponding meso form. This may reflect a slightly increased steric strain in the meso isomer. Elemental composition of each compound was confirmed by exact mass measurement of the molecular ion, which agreed with the predicted value usually within 10-ppm error.

The <sup>13</sup>C NMR spectra of the diastereomers of 2, 3, 4, and 5 are reported here for the first time and reveal important generalizations which may assist in the assignment of stereoisomer identity for other 3,4-disubstituted  $\gamma$ -diketones (Table II). The isomers exhibit small but significant differences in the chemical shifts for the carbonyl

(1) Presented at the 36th Southeastern Regional Meeting of the American Chemical Society, Raleigh, NC, 1984.

(2) Graham, D. G.; Anthony, D. C.; Boekelheide, K.; Maschmann, N. A.; Richards, R. G.; Wolfram, J. W.; Shaw, B. R. *Toxicol. Appl. Pharmacol.* 1982, 64, 415.

(3) Anthony, D. C.; Boekelheide, K.; Graham, D. G. *Toxicol. Appl. Pharmacol.* 1983, 71, 362. Anthony, D. C.; Boekelheide, K.; Anderson, C. W.; Graham, D. G. *Toxicol. Appl. Pharmacol.* 1983, 71, 372.

(4) Paal, C. *Chem. Ber.* 1884, 17, 2756. Knorr, L. *Chem. Ber.* 1884, 17, 2863. We are delighted to commemorate the centennial of these publications.

(5) Wolf, A. Ger. Pat. 876 237, 1953.

(6) Kharasch, M. S.; McBay, H. C.; Urry, W. H. *J. Am. Chem. Soc.* 1948, 70, 1269.

(7) Criege, R.; Noll, K. *Liebigs Ann. Chem.* 1959, 627, 1.

(8) Chkir, M.; Lelandais, D.; Bacquet, C. *Can. J. Chem.* 1981, 59, 945.

**Table I. Preparation and Physical Properties of  $\gamma$ -Diketones**

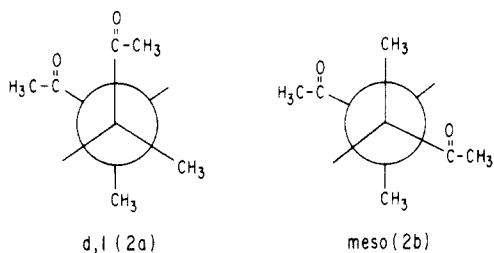
$\gamma$ -diketone	overall yield of diastereomer mixture, %	method <sup>a</sup> of separation of diastereomers	yield of diastereomer, %	bp, °C/mm	lit. bp, °C/mm	mp, °C	lit. mp, °C	$t_R$ on GC, <sup>e</sup> min
<b>2a</b>	61	A	30	25–29/0.05	52–53/2.5 <sup>7</sup>	<i>f</i>		6.8
<b>2b</b>			23	30–31/0.05	57–59/2.5 <sup>7</sup>	<i>f</i>		7.2
<b>3a</b>	63	B	24	38–41/0.05	112–115/20 <sup>18</sup>	<i>f</i>		10.2
<b>3b</b>			16	42–45/0.05		40–42 <sup>b</sup>		10.8
<b>4a</b>	62	B	29	50–55/0.05	80–85/4 <sup>19</sup>	22–23		11.5
<b>4b</b>			18	<i>f</i>		73–74 <sup>b</sup>		12.1
<b>5a</b>	<i>f</i>	C	11	147–167/0.5		102–104 <sup>c</sup>	103–105 <sup>d,14</sup>	10.5
<b>5b</b>			13	<i>f</i>		204–206 <sup>c</sup>	205–207 <sup>c,14</sup>	11.2

<sup>a</sup>Method A: column chromatography on a 230–400-mesh silica gel column, eluting with *n*-hexane:acetone (3:1). Method B: fractional distillation using stainless steel Heli-Pack column filling (Reliance Glass Works). Method C: fractional crystallization from ethyl ether:*n*-pentane (1.1). <sup>b</sup>From *n*-pentane. <sup>c</sup>From benzene. <sup>d</sup>From petroleum ether. <sup>e</sup>Retention time on gas chromatography (see Experimental Section for conditions). *f*Not determined.

**Table II. <sup>13</sup>C Chemical Shifts of *d,l* (a) and Meso (b) Diastereomers of  $\gamma$ -Diketones<sup>a</sup>**

$\gamma$ -diketone	C-1,6	C-2,5	C-3,4	C-7,8	C-9,10	C-9',10'
<b>2a</b>	28.3	211.5	48.1	13.3		
<b>2b</b>	28.8	210.4	48.5	14.4		
<b>3a</b>	29.8	211.4	51.5	20.5	9.7	
<b>3b</b>	30.0	210.1	54.8	22.9	10.9	
<b>4a</b>	26.2	212.1	55.8	33.7	22.0	16.6
<b>4b</b>	28.4	210.0	56.4	34.2	22.1	17.4
<b>5a<sup>b</sup></b>	29.2	207.7	61.8			
<b>5b<sup>b</sup></b>	30.4	206.0	60.8			

<sup>a</sup>ppm from Me<sub>4</sub>Si in CDCl<sub>3</sub>. <sup>b</sup>Excluding phenyl carbons.

**Figure 1.** Newman projections showing preferred conformation for *d,l* (a) and meso (b) diastereomers of 3,4-dimethylhexane-2,5-dione (2).

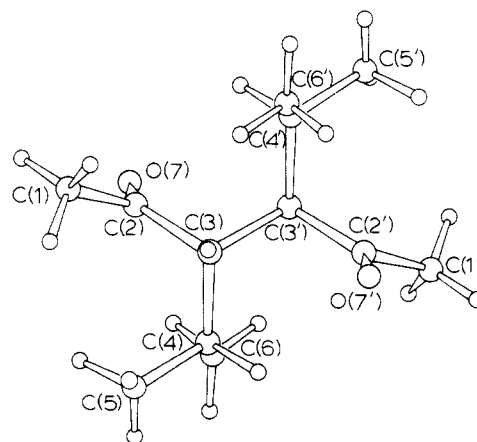
carbons (C-2,5) and the carbon substituent (C-7,8) on the 3,4-positions; in every case, the carbonyl carbon is more shielded in the meso isomers, while C-7,8 is more shielded in the *d,l* isomers. Since these carbons are  $\gamma$ -related to each other, the shift effects may arise from the conformational differences in the isomers, illustrated in Figure 1 for the 3,4-dimethyl isomers (2a,b). In the meso isomer the carbonyls are gauche to the methyl groups but in the *d,l* isomer the carbonyls are gauche to each other. Methyl, therefore, appears to exert a greater shielding effect on carbonyl than does the other carbonyl group. In the *d,l* isomer, the two methyls are gauche to each other and are more shielded than in the meso isomer, where methyl has a gauche interaction with the carbonyl group. The chirality at C-3,4 makes the two methyl groups diastereotopic in the 3,4-diisopropyl compounds (4a,b) and they therefore have different chemical shifts.

Additionally, single-crystal X-ray analysis defined the structure of **4b** unequivocally. The crystal structure was

**Table III. Fractional Atomic Coordinates<sup>a</sup> ( $\times 10^4$ ;  $\times 10^3$  for H) and Thermal Parameters ( $\text{\AA}^2$ ) for **4b** (with Standard Deviations in Parentheses)**

atom	<i>x</i>	<i>y</i>	<i>z</i>	<i>B</i> or <i>B<sub>eq</sub></i>
C (1)	7891 (3)	3924 (2)	2550 (4)	5.48 (5) <sup>b</sup>
C (2)	6781 (2)	2472 (2)	357 (3)	3.74 (3) <sup>b</sup>
C (3)	4946 (2)	903 (2)	684 (2)	3.24 (3) <sup>b</sup>
C (4)	2994 (2)	1107 (2)	-62 (3)	4.07 (3) <sup>b</sup>
C (5)	2842 (3)	2812 (2)	1473 (4)	5.49 (4) <sup>b</sup>
C (6)	2699 (3)	1028 (3)	-2730 (3)	6.15 (5) <sup>b</sup>
O (7)	7338 (2)	2538 (2)	-1627 (2)	5.51 (3) <sup>b</sup>
H (1A)	912 (4)	501 (4)	241 (5)	9.7 (8)
H (1B)	843 (4)	333 (3)	347 (5)	8.4 (7)
H (1C)	697 (3)	434 (3)	334 (4)	7.9 (6)
H (3)	500 (2)	101 (2)	246 (3)	3.9 (3)
H (4)	183 (3)	1 (2)	24 (3)	4.4 (4)
H (5A)	167 (4)	289 (4)	119 (5)	9.7 (8)
H (5B)	398 (3)	400 (3)	133 (4)	6.9 (6)
H (5C)	316 (4)	296 (3)	326 (5)	8.0 (6)
H (6A)	148 (3)	110 (3)	-306 (4)	6.5 (5)
H (6B)	283 (3)	1 (3)	-367 (4)	7.3 (6)
H (6C)	371 (3)	194 (3)	-320 (4)	7.8 (6)

<sup>a</sup>Hydrogen atoms bear the same labels as the carbon atoms to which they are bonded. <sup>b</sup>Anisotropically refined atoms;  $B_{eq} = 1/3(\beta_{11}a^2 + \beta_{22}b^2 + \beta_{33}c^2 + \beta_{12}ab \cos \gamma + \beta_{13}ac \cos \beta + \beta_{23}bc \cos \alpha)$ .

**Figure 2.** Structure and solid-state conformation of **4b**; small circles denote hydrogen atoms.

solved routinely by direct methods.<sup>9</sup> Full-matrix least-squares refinement of atomic parameters converged to  $R = 0.055$ <sup>10</sup> over 958 reflections measured by diffractometer. Final atomic positional parameters are in Table III. A

(9) Main, P.; Lessinger, L.; Woolfson, M. M.; Germain, G.; Declercq, J.-P. "MULTAN76, A System of Computer Programmes for the Automatic Solution of Crystal Structures"; Universities of York and Louvain, 1976.

(10)  $R = \sum ||F_o| - |F_c|| / \sum |F_o|$ .

**Table IV. Kinetics of Pyrrole Formation in the Reaction between  $\gamma$ -Diketones and Benzylamine**

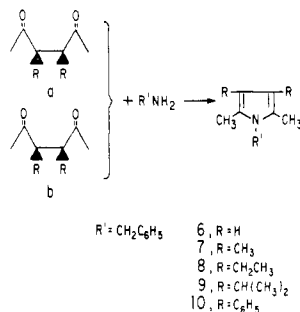
$\gamma$ -diketone	pseudo-first-order rate constant, s <sup>-1</sup>	correln coeff <sup>a</sup>
1	$5.19 \times 10^{-5}$	0.999
2a	$4.42 \times 10^{-4}$	0.994
2b	$7.56 \times 10^{-5}$	0.993
3a	$1.29 \times 10^{-5}$	0.970
3b	$2.86 \times 10^{-6}$	0.997
4a	$3.69 \times 10^{-7}$	0.990
4b	$2.63 \times 10^{-8}$	0.972
5a	$3.42 \times 10^{-6}$	0.999
5b	$4.06 \times 10^{-7}$	0.997

<sup>a</sup> Initial rates were determined by linear regression analysis, with calculation of the correlation coefficient in each case.

view of the solid-state conformation is presented in Figure 2. Interatomic distances, bond angles, and torsion angles are available in the supplementary material.<sup>11</sup> Crystals of 4b comprise discrete centrosymmetric molecules separated by van der Waals distances. Although the mean C<sub>sp<sup>2</sup></sub>-C<sub>sp<sup>3</sup></sub> bond length at 1.536 Å is very close to the expected value<sup>12</sup> (1.537 Å), the contributing members may be subdivided into two classes according to the degree of substitution at the carbon centers involved. Thus, the mean of the distances between only secondary carbon centers (1.550 Å) is significantly greater than that between primary and secondary centers (1.522 Å). Other distances and angles are not unusual.

The synthesis of pyrroles in this study followed the usual method<sup>13</sup> of condensing  $\gamma$ -diketones with benzylamine as the model amine except that excess benzylamine was used instead of solvent. The <sup>13</sup>C NMR, <sup>1</sup>H NMR, and mass spectral data for the pyrroles are provided in the supplementary material.<sup>11</sup> The pyrroles are characterized by molecular ions of high relative abundance and a prominent ion at *m/z* 91 derived from the benzyl group. Elemental composition was confirmed by accurate mass determination as previously described for the diketones.

The <sup>1</sup>H NMR spectra disclose that the pyrrole ring causes upfield shifting of the ortho protons of the benzyl group. The phenyl protons of benzyl groups usually appear as a singlet (as seen in benzylamine), while for the pyrroles 6-10, there was clear distinction between a 2 H multiplet



at 6.7-7.0 ppm and a 3 H multiplet at 7.0-7.4 ppm. This effect may arise from passage of the ortho protons through the shielding region of the pyrrole ring.

The kinetics of reaction with benzylamine were determined for the nine  $\gamma$ -diketones. The exact mechanism of the Paal-Knorr reaction is not known, nor is the identity of the rate-limiting step. We used the rate of appearance of the pyrrole product to determine the substituent effects on the overall reaction rate. As presented in Table IV, the rate of pyrrole formation was always greater for the *d,l*

than the meso diastereomer, 4-6-fold for 2 and 3, and over 14-fold for 4. The *d,l* diastereomer may react faster than the meso because of lesser interaction between substituents in the attainment of the planar conformation required for ring formation. While 3,4-dimethyl substitution accelerated the Paal-Knorr reaction, its rate was reduced by the larger substituents relative to the rate seen for 1. Differences in steric interactions (or electronic effects) in the various species involved in this complex process may be responsible for this rate effect. In any case, these results clearly demonstrate the importance of steric effects in the starting  $\gamma$ -diketones on the rate of pyrrole formation. As will be reported separately, 2a was more neurotoxic than 2b, when given to rats, apparently reflecting the greater rate of pyrrole formation in vivo.

## Experimental Section

**General Methods.** Proton NMR spectra were recorded on an IBM Fourier Transform NR-80 spectrometer, and proton-decoupled carbon-13 NMR spectra were obtained at 22.5 MHz with a JEOL FX 90 Q spectrometer. All NMR data were taken in chloroform-*d* with tetramethylsilane (Me<sub>4</sub>Si) as internal standard.

Mass spectra were performed with a VG 7070E-11/250 double-focusing mass spectrometer-data system combination, operated in EI mode (acceleration voltage 5 kV, electron energy 70 eV, trap current 100  $\mu$ A, resolution 1500). GC/MS analyses were performed by split-injection on a fused-silica capillary GC column, 30 m  $\times$  0.25 mm internal diameter, coated with a chemically bound methyl silicone (DB-1, J&W Scientific, Rancho Cordova, CA). The GC oven temperature was programmed from 130  $^{\circ}$ C to 200  $^{\circ}$ C at 10 $^{\circ}$ /min. The mass range 600-20 was scanned at 1 s/decade. Accurate mass measurements were performed by peak matching at a resolution of about 6000 (10% valley definition) using ions from perfluorokerosene for internal reference. Samples were introduced using the direct insertion probe.

Analytical gas chromatography was performed with a Varian S1400 gas chromatograph equipped with a flame-ionization detector using nitrogen as the carrier gas at 30 mL/min. For analysis of 3,4-disubstituted  $\gamma$ -diketones, column temperature was programmed from 100  $^{\circ}$ C to 200  $^{\circ}$ C at 10 $^{\circ}$ /min with injector temperature 140  $^{\circ}$ C, and detector temperature 240  $^{\circ}$ C. For pyrrole analysis, the column temperature was 240  $^{\circ}$ C, injector temperature was 255  $^{\circ}$ C, and detector temperature was 270  $^{\circ}$ C. The analysis of  $\gamma$ -diketones employed a 2-m Varian prepac column of 3% OV-101 on 80/100-mesh Chromosorb W-HP; for the pyrroles, a 10% OV-101 on 80/100-mesh Chromosorb W-HP was used.

Analytical high-performance liquid chromatography (HPLC) was conducted with a Perkin-Elmer Series 4 liquid chromatograph with a Perkin-Elmer silica column P-E HS-5, 4.6  $\times$  150 mm, and a Perkin-Elmer LC-95 variable wavelength detector set at 217 nm. Pyrroles were eluted with 2-propanol-cyclohexane (2:98) at a 1 mL/min flow rate. Pyrroles were eluted between 1.6 and 2.1 min, after which unreacted starting materials were eluted from the column with 2-propanol. Concentrations of pyrrole were determined from calculations of areas under peaks with a Perkin-Elmer LCI 100 Laboratory Computing Integrator.

The source of 2-butanone (99%), 4-methyl-2-pentanone (99.5%), 2-pentanone (97%), benzylamine (99%), and 1 was Aldrich Chemical Company. Phenylacetone (technical) was purchased from Sigma Chemical Company and cyclohexane (HPLC/spectro-grade) from Pierce Chemical Company. All reactants were freshly distilled before use. Technical lead dioxide (PbO<sub>2</sub>) was obtained from Fisher Chemical Company. Boiling and melting points are uncorrected.

**Dehydrodimerization Reactions.** Using a modification of a published procedure,<sup>5</sup> the dehydrodimerizations of 2-butanone, 2-pentanone, and 4-methyl-2-pentanone were carried out in a 30  $\times$  90 mm Soxhlet extraction apparatus equipped with a 25  $\times$  90 mm cellulose extraction thimble (Whatman) containing 100 mmol of PbO<sub>2</sub> mixed with 20 g of sand. The ketone (1.5 mol) was refluxed through the thimble for 18-24 h; excess starting material was then removed with a rotary evaporator, and the products were distilled at 0.05-0.1 mm. Diastereomers 2a and 2b were separated

(11) Supplementary material, see paragraph at end of paper.

(12) *Chem. Soc. Spec. Publ.* 1965, 18.

(13) Wolthuis, E.; Jagt, D. V.; Mels, S.; DeBoer, A. *J. Org. Chem.* 1965, 30, 190.

by column chromatography (method A, Table I), while fractional distillation was used to separate **3a** from **3b** and **4a** from **4b** (method B, Table I).

The dehydrodimerization of phenylacetone (200 mmol) was effected with  $\text{PbO}_2$  (100 mmol) in benzene (100 mL) with mechanical stirring for 1 h at reflux temperature. The filtered mixture was then concentrated by rotary evaporation and the residue crystallized fractionally (method C, Table I) by stirring with 100 mL of ethyl ether-*n*-pentane (1:1) at 30 °C. On cooling in a dry ice bath, **5b** separated as white crystals and was recrystallized from benzene. The **5a** diastereomer was distilled from the filtrate of **5b** between 147 °C and 167 °C at 0.5 to 1.0 mm, yielding a dense oil which readily crystallized. It was recrystallized from benzene. The  $^1\text{H}$  NMR and mass spectra for each are available as supplementary material.<sup>11</sup> The  $^{13}\text{C}$  NMR data are in Table II.

**Paal-Knorr Synthesis of Pyrroles.**<sup>13</sup> The  $\gamma$ -diketones (20 mmol), either pure 1 or mixtures of *d,l* and meso diastereomers of **2**, **3**, **4**, and **5**, were stirred with 200 mmol of benzylamine at 50–60 °C for 24 h under Ar atmosphere. Then the excess benzylamine was distilled at 0.5 mm and the residue stirred with 5–10 mL of 95% ethanol at room temperature under Ar and cooled in a dry ice bath to crystallize the pyrroles. The pyrroles were recrystallized from 95% ethanol; mmol, yield, mp for each are given below. The  $^{13}\text{C}$  NMR,  $^1\text{H}$  NMR, and mass spectral data are given as supplementary material.<sup>11</sup>

**1-Benzyl-2,5-dimethylpyrrole (6):** 9.6 mmol; 48%; mp 43–44 °C [lit.<sup>13</sup> mp 45–45.3 °C, lit.<sup>15</sup> mp 43 °C].

**1-Benzyl-2,3,4,5-tetramethylpyrrole (7):** 12 mmol; 60%; mp 23–24 °C (lit.<sup>16</sup> mp 21–21.5 °C).

**1-Benzyl-3,4-diethyl-2,5-dimethylpyrrole (8):** 13 mmol; 65%; mp 48–49 °C.

**1-Benzyl-3,4-diisopropyl-2,5-dimethylpyrrole (9):** 9.8 mmol; 49%; mp 70–71 °C.

**1-Benzyl-3,4-diphenyl-2,5-dimethylpyrrole (10):** 15 mmol, 75%, mp 145–146 °C [lit.<sup>17</sup> mp 147–149 °C].

**Kinetics of Pyrrole Formation.** The Paal-Knorr reactions were carried out in an Ar atmosphere in cyclohexane at a molar rate of 1:20 ( $\gamma$ -diketone to benzylamine) and a  $\gamma$ -diketone concentration of 10 mM. The reaction mixtures were stirred magnetically at  $30 \pm 0.05$  °C with a Haake Series F constant temperature circulator. At timed intervals aliquots were withdrawn for HPLC analysis. Pseudo-first-order rate constants were calculated from the slope of  $\ln [A_0]/([A_0] - [X])$  vs time where  $[A_0]$  = initial concentration of diketone (10 mM) and  $[X]$  = concentration of the pyrrole at each time point.

**Single-Crystal X-ray Structure Determination of 4b.**  $\text{C}_{12}\text{H}_{22}\text{O}_2$  (**4b**), mol wt 198.31, triclinic,  $a = 7.230$  (1) Å,  $b = 8.282$  (1) Å,  $c = 5.724$  (1) Å,  $\alpha = 103.69$  (1)°,  $\beta = 90.03$  (1)°,  $\gamma = 111.88$  (1)°,  $V = 307.5$  Å<sup>3</sup>,  $Z = 1$ ,  $D_{\text{calc}}$  = 1.071 g cm<sup>-3</sup>,  $\mu$ (Cu K $\alpha$  radiation,  $\lambda = 1.5418$  Å) = 5.2 cm<sup>-1</sup>. Space group  $P1(C^1_1)$  or  $P1(C^1_1)$  from

Laue symmetry; shown to be the latter by structure solution and refinement.

A crystal of dimensions ca. 0.20 × 0.40 × 0.64 mm was sealed inside a thin-walled glass capillary. Oscillation, Weissenberg, and precession photographs yielded preliminary unit-cell parameters and space group information. Intensity data were recorded on an Enraf-Nonius CAD-4 automated diffractometer (Cu K $\alpha$  radiation, incident-beam graphite monochromator;  $\omega$ - $2\theta$  scans,  $\theta_{\text{max}}$  67°). From a total of 1090 independent measurements, those 958 reflections with  $I > 3.0\sigma(I)$  were retained for the structure analysis and corrected for the usual Lorentz and polarization effects. Refined unit-cell parameters were derived by least-squares treatment of the diffractometer setting angles for 25 high-order ( $56^\circ < \theta < 67^\circ$ ) reflections widely separated in reciprocal space.

The crystal structure was solved by direct methods.<sup>9</sup> Approximate non-hydrogen atom coordinates were obtained from an *E* map. Full-matrix least-squares adjustment of atomic positional and anisotropic thermal parameters reduced *R* to 0.120.<sup>10</sup> Hydrogen atoms were then located in a different Fourier synthesis, and their positional and isotropic thermal parameters were included as variables in all subsequent full-matrix least-squares iterations which converged to  $R = 0.055$ .<sup>10</sup>

Final atomic positional parameters are in Table III. Anisotropic temperature factor parameters are available in the supplementary material.<sup>11</sup>

Neutral atom scattering factors used in the structure-factor calculations were taken from ref 20. In the least-squares iterations,  $\Sigma w\Delta^2$  ( $\Delta = ||F_o| - |F_c||$ ) was minimized with weights,  $w$ , assigned according to the scheme:  $w^{1/2} = 1$  for  $|F_o| < 2.6$ , and  $w^{1/2} = 2.6/|F_o|$  for  $|F_o| > 2.6$  to ensure no systematic dependence of  $\langle w\Delta^2 \rangle$  when analyzed in ranges of  $|F_o|$ .

**Acknowledgment.** We gratefully acknowledge the preparation of  $^1\text{H}$  and  $^{13}\text{C}$  NMR spectra by Brian G. Marsi. This work was supported by NIH Grant 2R01 ES02611 to Dr. Graham and by NIH Training Grant 5T32 AG00007 to Dr. F. S. Vogel.

**Registry No.** **1**, 110-13-4; **2a**, 28895-03-6; **2b**, 28895-02-5; **3a**, 34506-20-2; **3b**, 34506-19-9; **4a**, 99902-11-1; **4b**, 99902-10-0; **5a**, 69373-32-6; **5b**, 69373-33-7; **6**, 5044-20-2; **7**, 3469-21-4; **8**, 99902-12-2; **9**, 99902-13-3; **10**, 79823-43-1;  $\text{C}_6\text{H}_5\text{CH}_2\text{NH}_2$ , 100-46-9;  $\text{CH}_3\text{COC}-\text{H}_2\text{CH}_3$ , 78-93-3;  $\text{CH}_3\text{COCCH}_2\text{CH}_3$ , 107-87-9;  $\text{CH}_3\text{COCCH}_2\text{CH}(\text{CH}_3)_2$ , 108-10-1;  $\text{CH}_3\text{COCCH}_2\text{Ph}$ , 103-79-7.

**Supplementary Material Available:** Table V, proton NMR and mass spectral data for diketones and pyrroles; Table VI,  $^{13}\text{C}$  NMR shifts of substituted pyrroles; Table VII, anisotropic temperature factor parameters for **4b**; Table VIII, interatomic distances and angles in **4b**; Table IX, torsion angles in **4b** (8 pages). Ordering information is given on any current masthead page.

(14) Hawkins, E. G. E.; Large, R. *J. Chem. Soc. Perkin Trans. 1* 1974, 2, 280.

(15) Patterson, J. M.; Soedigo, S. *J. Org. Chem.* 1968, 33, 2057.

(16) Wolthuis, E.; DeBoer, A. *J. Org. Chem.* 1965, 30, 3225.

(17) Meyer, H. *Liebigs Ann. Chem.* 1981, 9, 1534.

(18) Wolthuis, E.; Bossenbroek, B.; DeWall, G.; Geels, E.; Leegwater, A. *J. Org. Chem.* 1963, 28, 148.

(19) Lüdicke, M.; Wolf, A. *Z. Naturforsch. B* 1959, 14, 111.

(20) "International Tables for X-Ray Crystallography", Vol. IV, The Kynoch Press: Birmingham, England, 1974.

## Novel Construction of Penem Ring System from Penicillin Derivatives. Synthesis of 2-Carboxypenem Derivative<sup>1</sup>

Tetsuji Kametani,\* Naoaki Kanaya, Atsushi Nakayama, Tomoko Mochizuki, Shuichi Yokohama, and Toshio Honda

*Institute of Medicinal Chemistry, Hoshi University, Ebara 2-4-41, Shinagawa-ku, Tokyo 142, Japan*

Received July 19, 1985

6-Aminopenicillanic acid derivative **1** was successfully transformed into 2-carboxypenem derivative **15** by employing a carbene reaction of  $\alpha$ -diazoacetate as a key step.

It is now well established that penem derivatives are endowed with potent antibacterial activity. Development

of methodology for the construction of a penem ring system is therefore an important objective.<sup>2</sup> During the